

# Computational study of the anode baking industrial furnace

Prajakta Nakate<sup>1,2</sup>, Domenico Lahaye<sup>1</sup>, Cornelis Vuik<sup>1</sup>, Marco Talice<sup>3</sup>

<sup>1</sup>Delft University of Technology

Van Mourik Broekmanweg 6, 2628 XE, Delft, Netherlands

P.A.Nakate@tudelft.nl; D.J.P.Lahaye@tudelft.nl; C.Vuik@tudelft.nl; m.talice@pm2engineering.com

<sup>2</sup>Aluminium & Chemie (Aluchemie) Rotterdam B.V.

Oude Maasweg 80, 3197 KJ, Botlek, Netherlands

<sup>3</sup>PM2ENGINEERING, Cagliari, Italy

**Abstract** – In the aluminium industry, the Hall-Héroult process is used for smelting of aluminium using carbon electrodes such as anodes. The baking process of anodes is required for their maximum efficiency during this electrolysis process. The anode baking process contributes up to 15% costs in the aluminium industries and therefore, has been proven to be an important field of research since the 1980s. The process consists of various interdependent physics such as turbulent flow, combustion, radiation, and conjugate heat transfer. The ideal anode baking process should attempt to optimize energy consumption, reduce NO<sub>x</sub> and CO<sub>2</sub> emissions and improve anode quality. The focus of this project is to understand the parameters that affect thermal NO<sub>x</sub> production in the anode baking furnace and thereby, finding optimum values of these parameters.

In this paper, a 2D reactive turbulent flow model is developed using COMSOL<sup>®</sup> Multiphysics finite element software. The effects of radiation are elaborated for a 2D model. The temperatures calculated by the model are compared with the temperatures measured in the furnace using an infrared thermal camera. The comparison shows that the temperatures obtained by the model are in the range of measured temperatures. The combustion modeling is mixing dominated. A 3D model provides more accurate mixing behaviour. Therefore, an extension of the 2D model to 3D using COMSOL<sup>®</sup> Multiphysics software is developed. In this paper, results of 3D non-reactive turbulent flow results are discussed. Initially, mesh sensitivity of the 3D results is analysed by comparing three mesh refinement levels. Subsequently, the results are compared with another simulation environment, IB-Raptor code. The comparison shows that the differences in the results are mainly observed near the fuel pipe. These differences can be attributed to the dissimilarities in mesh size and structure. However, these differences are within a 10% range and therefore, the two codes can be considered to provide comparable results. An improvement in the comparison with the two tools can be achieved by increased consistency in meshing. Furthermore, a 3D non-reactive flow would be improved by implementing other important physical phenomena similar to the development of a 2D model.

**Keywords:** Turbulent flow, Eddy dissipation model, Combustion, NO<sub>x</sub>, Zeldovich mechanism

## 1. Introduction

Aluminium is extracted from bauxite ore using the Hall-Héroult process using electrolysis. The anodes used in the electrolysis process are one of the major components as it contributes to 15% of the total costs in aluminium production [1]. The baking of anodes is required before using them in the electrolysis process to have the desired properties of anodes. The baking process is carried out in open ring furnaces as shown in Figure 1. The anode baking process involves dependency of multiple physical phenomena such as turbulent flow, combustion process, radiation, and conjugate heat transfer. The heat generated by the combustion process is transferred through walls to the anodes. The conventional process needs improvement to reduce energy consumption and to reduce NO<sub>x</sub> and soot formation without degrading the quality of anodes. The current practices fail to achieve an optimized process. The ability of mathematical modeling to provide a better understanding of the process consisting of interdependent physical phenomena is vital.

Development of computational simulations of the industrial furnaces including combustion is in process since decades [2], [3]. The importance of computational simulation of an anode baking furnace was realized since the 1980s. Bui. et. al proposed a 1D model in 1983 based on a simple assumption that the process acts similar to a semi-continuous counter-flow heat exchanger [4], [5]. These relatively simple models form the basis of the models developed in the later stage. Significant work on modeling of the anode baking process was carried out afterwards by various authors that focus on improving models [6]–[11]. However, though these models are useful for designing purpose and understanding the process, they are limited by their inability to predict NO<sub>x</sub> and soot formation. Recently, Bourgier et. al. developed a model that provides insights on the 3D transient model of the entire fire-line developed in ANSYS Fluent software by taking into account all important physical phenomena [12]. However, improvements in the model are needed to implement control strategies, predict soot and NO<sub>x</sub> formation. The most recent model by Tajik et. al. [12] studies the effect of diluted oxygen at elevated air temperature to implement moderate or intense low-oxygen dilution (MILD) combustion. The effect of these key features of MILD combustion on NO<sub>x</sub> formation are discussed and the optimized dilution level is provided [12]–[14]. However, the validation of the model at different modeling steps is obscure.

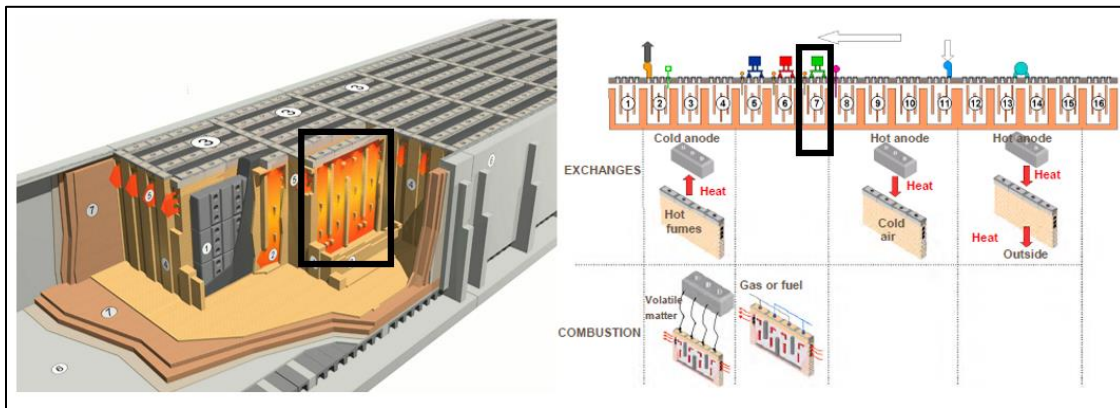


Figure. 1: (Left) Schematic of anode baking furnace and (Right) 2D overview of various sections of anode baking furnace. The model of highlighted section is studied in this work (© 2011 RIO TINTO ALCAN INC., PRIMARY METAL)

Aluchemie Rotterdam B.V., is working on reducing the NO<sub>x</sub> from the anode baking furnace. The mathematical modeling is helpful to optimize the process in terms of reducing NO<sub>x</sub>. The project aims to obtain a validated mathematical model of the heating section of the anode baking furnace. The choice of this heating section is based on the involvement of all major physics that affect NO<sub>x</sub> in the furnace. In the previous paper [15], a 2D model of the heating section is elaborated. However, the model is not advanced in terms of radiation. In this paper, the effect of an upgraded radiation model is provided. The improvement in the radiation model also translates into the more reliable NO<sub>x</sub> distribution. The overall 2D model needs to be validated and therefore, preliminary temperature measurements are carried out in the furnace using an infrared thermal camera. The measured temperatures are compared with the temperatures calculated using the model. The comparison shows that the values are within a range of roughly 10%. The necessity of improving the model from 2D to 3D is also mentioned in the previous paper [15]. A 3D non-reactive flow is modeled and compared with another simulation environment, IB-Raptor code, which is developed by PM2ENGINEERING. The analysis on the comparisons of various parameters such as temperature, density, and velocity is carried out. The difference in the results is within a range of 10-15% which can be attributed to the dissimilarities in the mesh size and structure. The mesh sensitivity analysis of COMSOL<sup>®</sup> Multiphysics results is also elaborated. It can be observed that though there are slight differences in the results produced by the two tools, the flow patterns are comparable. However, consistent mesh refinement is required to achieve a closer comparison with the two simulation platforms.

## 2. Modeling and Simulation details

A continuous exchange of heat occurs between the fume gas and anodes in anode baking furnace through a wall. The heat exchange is indirect and the process acts like a counter-flow heat exchanger. The anode baking process is divided into four zones based on the direction of heat exchange; either from hot gas or hot anodes. These four zones in the process are preheating, heating, blowing and cooling zone. The limited computational power restricts the modeling of the complete anode baking furnace. Therefore, in this paper, focus is given on modeling one of the sections from the heating zone. The selected section from the heating zone contains all important physics that has an impact on NO<sub>x</sub> formation in the process. Figure 2 (a) and (b) show the studied section from the anode baking furnace which is transformed into the 2D geometry and 3D geometry model respectively. The studied section is shown in Figure 1 by the highlighted box.

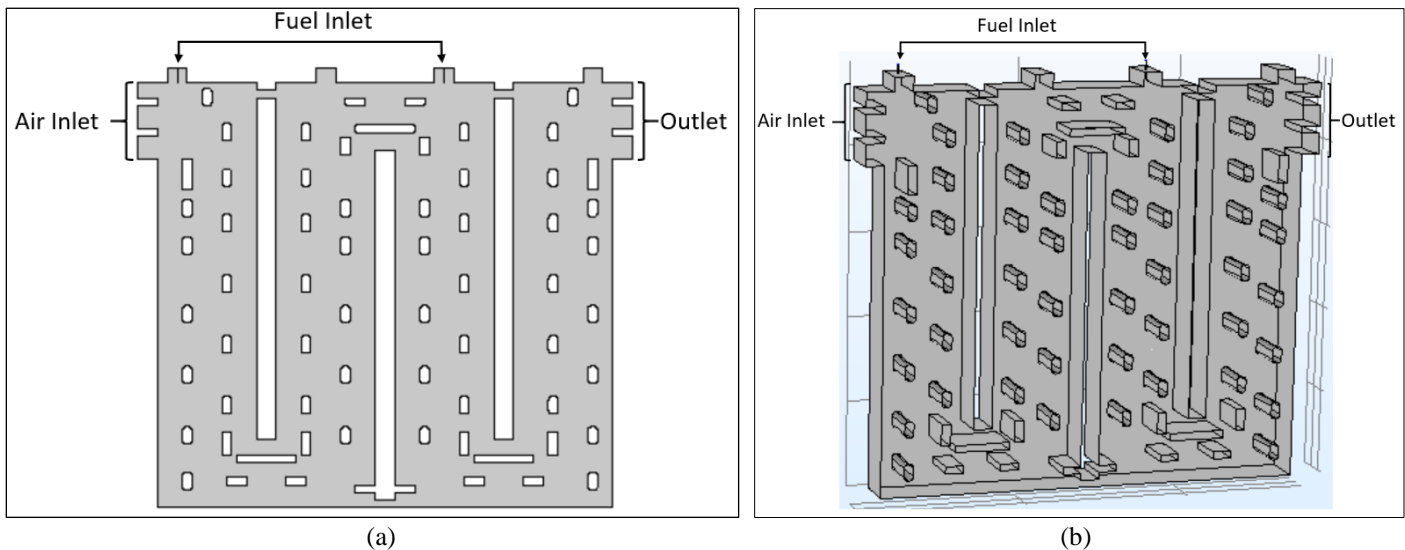


Figure. 2: (a) Geometry of 2D model of heating section in anode baking furnace (b) Geometry of 3D model of heating section in anode baking furnace

The modeling approach employed in this work consists of systematic development of the 2D model by gradually increasing the complexity of the model by adding physics in succession. The turbulent flow is modeled by considering a simplified time-averaged Navier-Stokes equation (RANS). The realizable  $k-\epsilon$  model is used for closing the Reynolds stress in the RANS equation [16]. The turbulence fluctuation is assumed not to affect the density and therefore, incompressible turbulent flow is considered. The density is defined by the equation of state. The exact equations used in the modeling are elaborated in the previous paper [15]. Wall functions are used as the boundary conditions at the walls. The combustion of methane is modeled by using the eddy dissipation model [16], [17]. Five chemical species, namely; CH<sub>4</sub>, O<sub>2</sub>, CO<sub>2</sub>, H<sub>2</sub>O, and N<sub>2</sub> are considered with single-step combustion reaction of CH<sub>4</sub>. As the eddy dissipation model assumes infinitely fast reaction, the intermediate endothermic reaction of formation of CO<sub>2</sub> from CO is not considered. Therefore, the computed temperature is assumed to be over predicted. The combustion modeling with mixture fraction/pdf model is in progress to correct this over prediction and will be presented in future [16], [17]. The process consists of the transport of heat by the gas streams as well as the generation of heat due to the combustion reaction. A piecewise cubic interpolation function and the thermodynamic data from literature are used to calculate the specific heat capacities of all the chemical species. The heat source is defined based on the enthalpy and progress of reaction. Temperatures at the inlet of air and fuel are specified as the boundary conditions based on the data from the furnace. P1 approximation model is used for the modeling of radiation [18]. The plank mean absorption coefficients of H<sub>2</sub>O and CO<sub>2</sub> are calculated by assuming the 4<sup>th</sup> order Gaussian function. The mixture absorption coefficient is then calculated based on the mass fraction and individual absorption coefficient of radiation-absorbing species (H<sub>2</sub>O and CO<sub>2</sub>). The data from refractory walls is used for defining the interpolation function for the

emissivity of walls as a function of temperature. Black surfaces are assumed at the inlet and outlet boundary. A stabilized convection-diffusion equation is solved at the post-processing stage for gaining an understanding of NO<sub>x</sub>. The Zeldovich mechanism is used for defining the source term in the transport equation. An equilibrium assumption is used for calculating the O radical concentration whereas, the OH radical concentration is assumed to be negligible as the mixture is fuel lean.

A 2D model provides insights into the overall process. However, a 3D model is necessary for the accurate description of the process. The modeling approach for developing a 3D model is similar to that of the 2D model, i.e., systematic development of the model is carried out by adding physics sequentially. In this paper, for the 3D model, only the results of non-reactive turbulent flow are elaborated. Similar to a 2D model, Reynolds average Navier-Stokes (RANS) equation is used with a realizable k- $\epsilon$  model. However, instead of incompressible flow, the model is improved to a compressible flow model and the density is defined by the equation of state. As opposed to a 2D model, instead of adding combustion reaction as a next step, the heat transfer equation is coupled before the combustion process. Therefore, the heat transfer equation does not contain the source term yet. The temperatures at the inlet of air and fuel are specified based on the measurement data from the furnace. The thermal conductivity, specific heat capacity and the ratio of specific heats are defined as constants. The Reynolds number and Mach number are around 45000 and 0.22 with respect to the jet velocity and diameter, respectively.

The COMSOL<sup>®</sup> Multiphysics software is used for the modeling of the process. The software is based on the finite element approach [19] and is a powerful tool for the coupling of multiple physics. The numerical models are solved with a segregated approach which accelerates the convergence by dividing the different physics as a separate segregated step. The segregated approach consumes less memory and each iteration is relatively faster. Furthermore, the domain decomposition preconditioner is used for GMRES iterative solver for solving the 3D model. This provides the advantage of solving large domains at relatively less memory. Overall, the COMSOL<sup>®</sup> Multiphysics software provides robust algorithms for numerically solving models using the finite element approach.

### 3. Results and Discussion

The results of the numerical simulation of 2D and 3D model of the heating section of anode baking furnace are presented. In the first subsection, the results of the 2D model are discussed. These results are elaborated in the previous paper [15]. In this paper, the subsequent results on the effect of radiation are explained. Moreover, the temperature predicted by the 2D model is compared with the measurements from the furnace. In the second subsection, the non-reactive turbulent flow results in the 3D model are discussed. These results are compared with another simulation environment to validate the results.

#### 3.1. Numerical simulation results of 2D model

A complete 2D model consisting of all physical phenomena is developed by increasing complexity of the model in terms of physics. The qualitative analysis of the results suggests that the distribution of variables such as velocity, mass fractions of chemical species, temperature aligns with the expected physical behaviour [15]. The comparison of the velocity distribution for varying jet velocity as boundary condition shows that for the higher velocity (200 m/s), the jet is penetrated deeper and the reaction zone is spread wider as compared to the lower velocity of the jet (150 m/s). The subsequent effect of the jet velocities on temperature distribution is also verified. These results are explained in the previous paper [15]. In the previous paper, the effect of radiation is elaborated by using an assumption of plank mean absorption coefficient defined as 4<sup>th</sup> order Gaussian function. This model assumes a gray gas behaviour of radiation-absorbing species such as CO<sub>2</sub> and H<sub>2</sub>O. However, the literature suggests that this assumption is not valid for combustion product species such as CO<sub>2</sub> and H<sub>2</sub>O. Therefore, in a further step, the radiation model is improved.

The development of the radiation model is continued by assuming the non-gray behaviour of CO<sub>2</sub> and H<sub>2</sub>O. The weighted sum of gray gas (WSSG) model is incorporated by assuming four gray gases. The fitting parameters for the weighting factors and absorption coefficient used for the WSSG model are obtained from the literature [20]. Figure 3 compares the temperature distribution obtained by the model without radiation (Figure 3 (a)) with that of the model implementing radiation with WSSG model (Figure 3 (b)). The comparison shows that the temperature is uniformly distributed for the model that considers radiation as compared to the model without radiation. The hot spots observed in the model without radiation would eventually predict higher NO<sub>x</sub> formation as compared to the model that considers radiation. Moreover, due to the high-temperature zones

in the furnace, radiation is expected to be an important physical phenomenon. Therefore, radiation needs to be considered for better prediction of NO<sub>x</sub>.

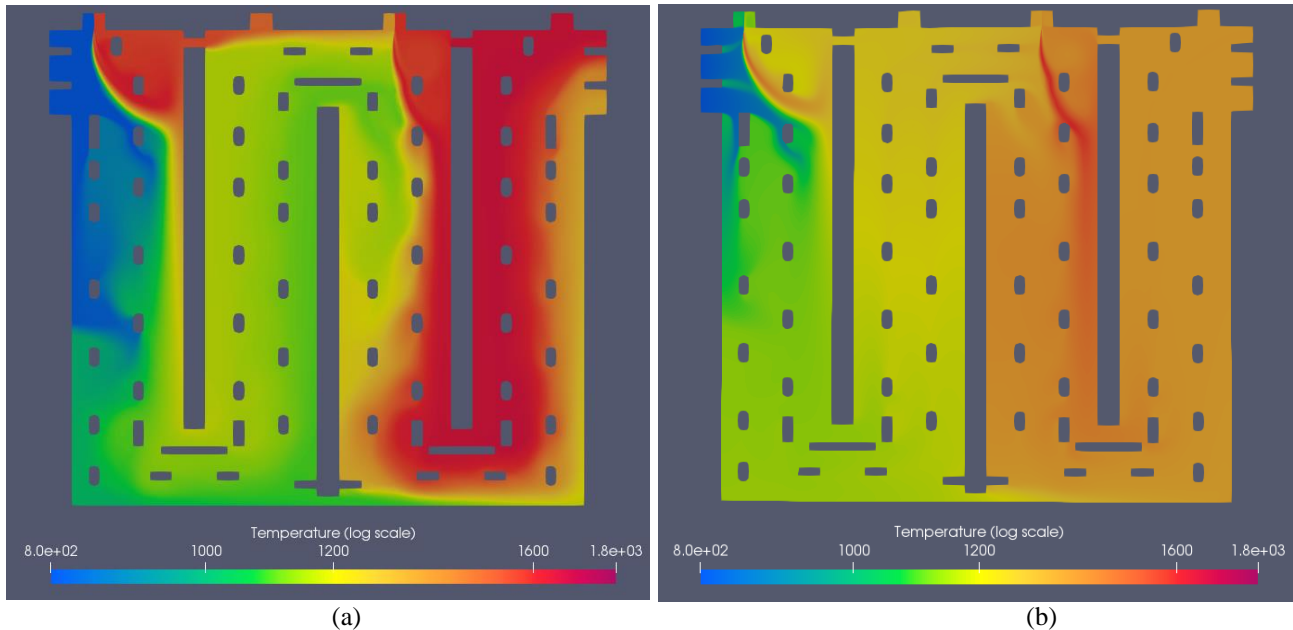


Figure. 3: (a) Temperature distribution obtained by the model without radiation (b) Temperature distribution obtained by assuming a WSSG non-gray gas radiation model

The measurement of the temperature in the furnace is carried out to have a basis for the validation of the model. This measurement aimed to check if the prediction of the temperature by the model is within a range of the temperature in the furnace. The temperatures are measured with a FLIR infrared thermal imaging camera. The infrared energy (radiation) is detected by these cameras and converted into an electronic signal. This signal is then processed to produce a thermal image which can be used to predict temperatures in heating chambers [21]. Figure 4 (a) shows the picture captured by the thermal camera by removing one of the burners from the furnace. The wall spotted in the image is expected to be the closest tie-brick in the furnace. The two images shown in Figure 4 (a) are captured in the same section of two different fire-lines. The temperature at the same tie-brick can be extracted from the model as well. Moreover, the temperatures at this tie-brick wall can be predicted by processing the thermal images captured by the camera. Note that the temperatures on the scale of figures in 4 (a) are in Fahrenheit. The average of the temperatures predicted by several such pictures (converted in °K) is compared with the temperature computed by the model. Figure 4 (b) compares the temperatures measured by the cameras and the temperatures calculated by the model on several number of points from the tie-brick wall closer to the burner. This comparison shows that there are significant differences between the temperatures predicted by the camera and the model. The differences can be attributed to the less accurate combustion model, 2D nature of the model, inconsistency in the inlet conditions as well as the absence of out of plane conjugate heat transfer. Moreover, the thermal camera also provides only a rough prediction of the temperature due to its limitation to sustain high temperatures. Due to this limitation, the camera can be hold only at a certain distance from the hot chamber. Nonetheless, the analysis shows that the prediction by both tools is within a range of roughly 10%. Further improvement in the model would be needed for reducing this difference.

### 3.2. Numerical simulation results of 3D model

The 2D model is limited by its ability to determine the accurate mixing behaviour as discussed in the previous paper [15]. The temperature comparison with measurements also suggests that the improvement in the model is needed in terms of dimensionality of the model for better judgement of temperature distribution. Therefore, successive development of the 3D

model is carried out. Similar to the development of the 2D model, the approach of developing a 3D model has been planned by gradually increasing the complexity in terms of physics. In this paper, non-reactive turbulent flow results of a 3D model are discussed.

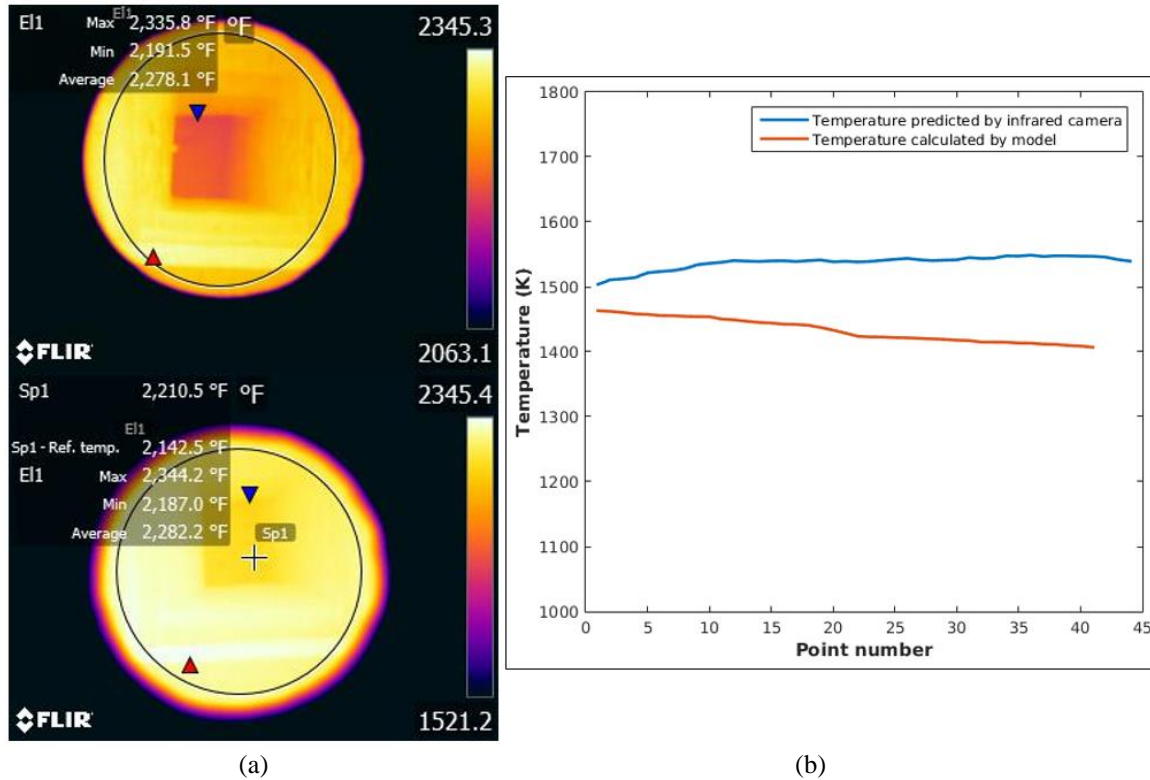


Figure 4: (a) Thermal images captured by the FLIR infrared camera from the burner inlet (b) Comparison of the temperature predicted by the thermal camera and the model on the same tie-brick wall near the burner

### 3.2.1 Mesh sensitivity analysis of numerical results of COMSOL® Multiphysics

A 3D non-reactive flow model is simulated with three refinement levels of mesh. The details of the statistics of the meshes are given in Table 1. The mesh is finer near the fuel inlet pipe as compared to the bulk domain in all three cases.

Table 1: Statistics of refinement levels of mesh implemented in 3D non-reactive flow model

Refinement level	Number of elements	Average element quality
Mesh Coarse (C)	850777	0.659
Mesh Medium (M)	1086068	0.662
Mesh Fine (F)	1400584	0.666

The temperature and velocity results are analysed with these three refinement levels on one horizontal line located near the fuel inlet on the XY center plane. Figure 5 (a) and (b) show the comparison of temperature and velocity on the abovementioned line for the different mesh levels. It can be observed from these comparisons that the maximum difference between the temperatures and velocities with the three refinements levels is approximately 42 K and 4 m/s, respectively. The differences are significant mostly in the region where the fuel pipe is located. A consistent trend of decreasing temperature or increasing velocity is not observed while increasing the refinement level. This might be due to the inconsistent refinement factor in the bulk domain and the domain near fuel inlet. In other words, the factor with which the mesh is refined in the bulk domain is different from the refinement factor in the region of fuel pipe. This can be improved by maintaining the consistency in the refinement. However, from an industrial perspective, the results can be claimed to be satisfactory.

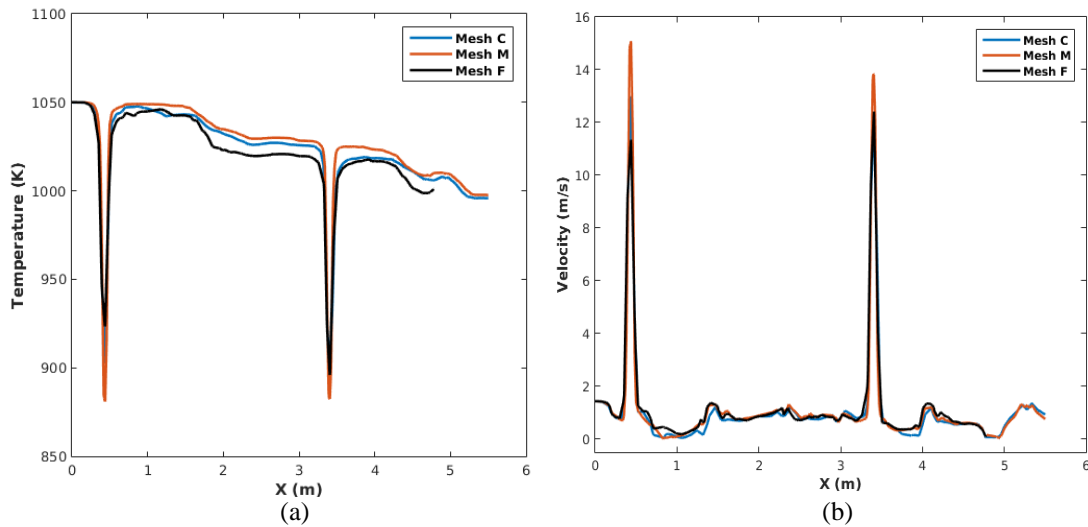


Figure. 5: (a) Comparison of temperature on line  $Y=4.5532\text{m}$  of XY center plane for three mesh refinement levels (b) Comparison of velocity on line  $Y=4.5532\text{m}$  of XY center plane for three mesh refinement levels

### 3.2.2 Comparison of numerical results obtained by COMSOL<sup>®</sup> Multiphysics and IB-Raptor code

The results obtained by COMSOL<sup>®</sup> Multiphysics are compared with another simulation environment to validate the results. The numerical simulation results for the 3D non-reactive turbulent flow model with the given boundary conditions are provided by PM2ENGINEERING with their IB-Raptor code. The solver of the code is based on a cell-centered finite volume discretization of the equations. The code utilizes IB-REX mesh generator which is based on immersed boundary condition [22]. The implementation of immersed boundary method results in a consistent Cartesian mesh as shown later in Figure 10. Figure 6 shows the comparison of temperature on the XY center plane simulated by the IB-Raptor code and COMSOL<sup>®</sup> Multiphysics. The preliminary observation shows that the temperature distribution in the bulk domain is comparable. For a precise comparison, the temperatures on the two lines (vertical and horizontal) presented in Figure 6 are plotted as a function of geometrical coordinates. It can be observed from Figure 7 (a) that the temperature estimated by COMSOL<sup>®</sup> Multiphysics is approximately 9% higher as compared to IB-Raptor code at the X coordinate where the burner pipe is located. Whereas, the differences in the results observed on the vertical line (Figure 7 (b)) varies slightly at the bottom of the furnace.

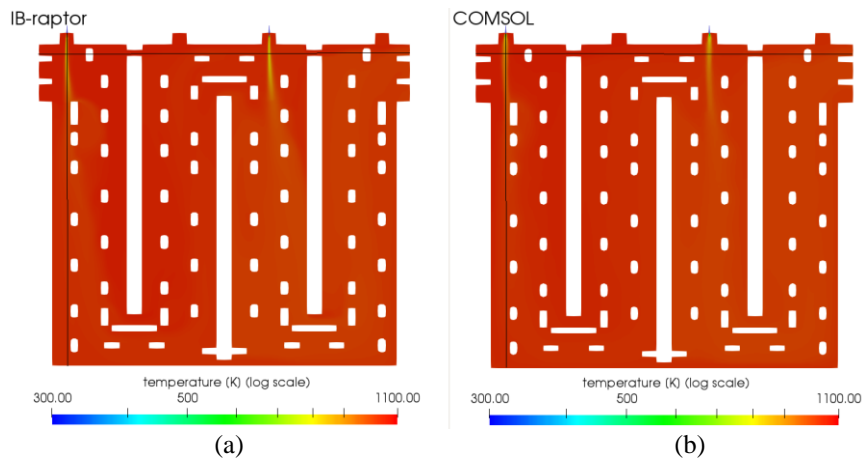


Figure. 6: (a) Color plot of temperature distribution obtained by IB-Raptor code on XY center plane (b) Color plot of temperature distribution obtained by COMSOL<sup>®</sup> Multiphysics on XY center plane

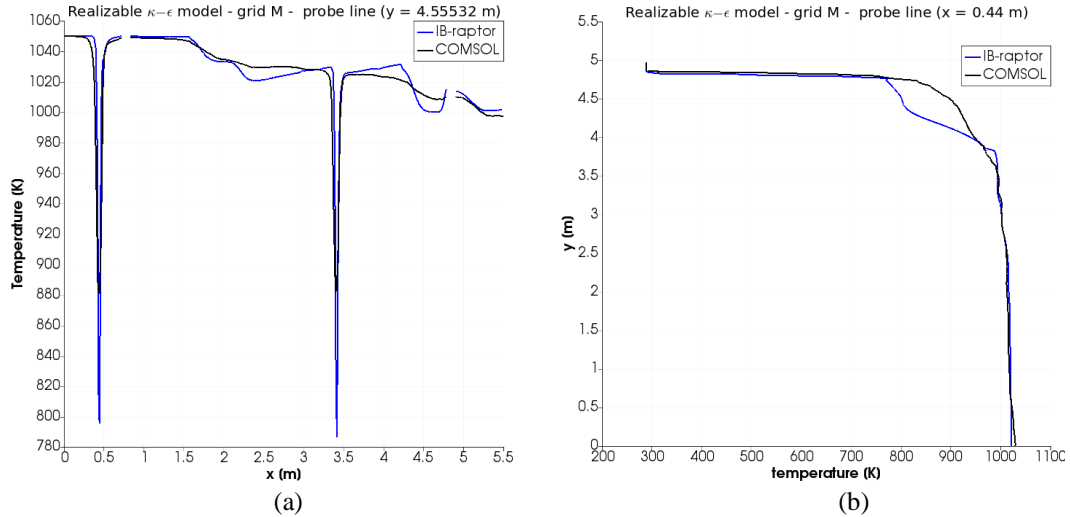


Figure 7: (a) Comparison of temperature on line Y=4.5532m of XY center plane with IB-Raptor code and COMSOL<sup>®</sup> Multiphysics (b) Comparison of temperature on line X=0.44 m of XY center plane with IB-Raptor code and COMSOL<sup>®</sup> Multiphysics

The density of the gas is modeled by employing the equation of state, i.e., the density is defined as a function of temperature. Therefore, the differences observed in Figure 7, between the temperatures calculated by two codes are translated into the density as well. The density near the jet location is observed to be lower with COMSOL<sup>®</sup> Multiphysics as compared to the IB-Raptor code. The flow is considered to be compressible and therefore, the velocities are dependent on the density of the gas. Figure 8 shows a comparison of velocity magnitude with COMSOL<sup>®</sup> Multiphysics and IB-Raptor code. The spreading of the jet is observed with COMSOL<sup>®</sup> Multiphysics near the outlet of the fuel pipe as opposed to the IB-Raptor code. A slight difference in the penetration of jet in the furnace is also observed. The occurrence of low-velocity zones is observed with both codes. However, the position of these zones does not overlap completely. Similar to the temperature, velocities are also compared on the same lines for more accurate comparison. It can be observed that the peak velocity near the location of fuel pipe obtained by COMSOL<sup>®</sup> Multiphysics differs by a magnitude of 3-4 m/s as compared to IB-Raptor code. The differences observed in the bulk domain are comparatively less significant.

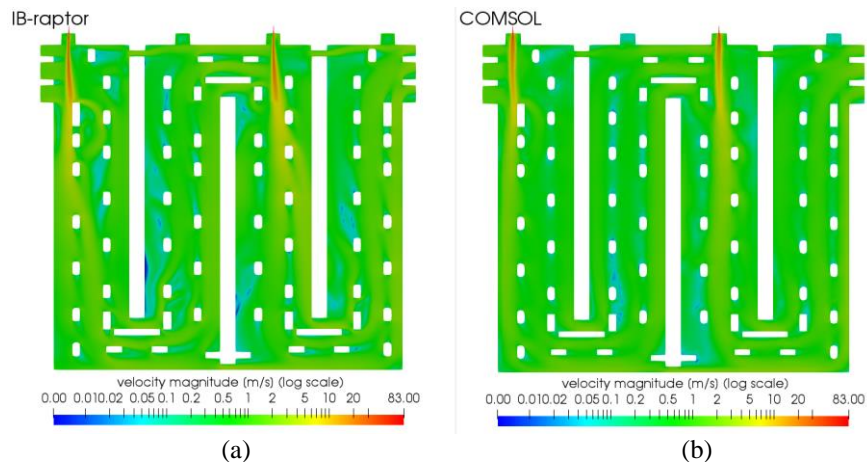


Figure 8: (a) Color plot of velocity distribution obtained by IB-Raptor code on XY center plane (b) Color plot of velocity distribution obtained by COMSOL<sup>®</sup> Multiphysics on XY center plane

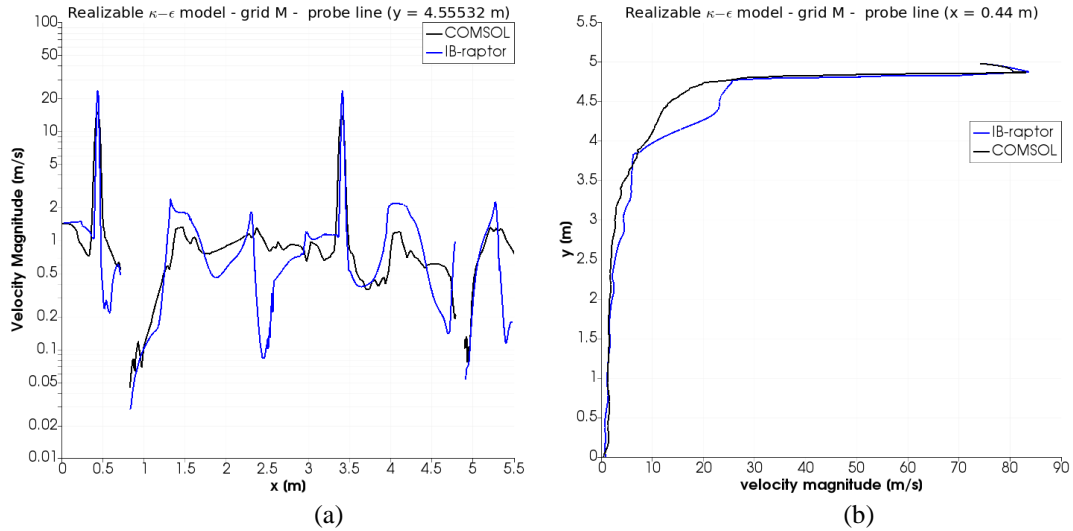


Figure. 9: (a) Comparison of velocity on line  $Y=4.55532\text{m}$  of  $XY$  center plane with IB-Raptor code and COMSOL Multiphysics (b) Comparison of velocity on line  $X=0.44\text{ m}$  of  $XY$  center plane with IB-Raptor code and COMSOL Multiphysics

### 3.2.3 Discussion on the numerical results obtained by COMSOL® Multiphysics and IB-Raptor code

The differences in the numerical results generated by the COMSOL® Multiphysics and IB-Raptor code are within 10-15% for the variables such as temperature and velocity near the fuel inlet pipe. Whereas, these differences are lower in the bulk flow region and the flow patterns observed by the two codes are comparable. These differences in the numerical results can be attributed to the dissimilarities in the discretization, type of solvers and the wall treatments to some extent. However, a detailed analysis shows that the disparity in the size and structure of the mesh has a major influence on the differences in the results.

Figure 10 shows the differences in the mesh implemented by COMSOL® Multiphysics and IB-Raptor code near the location of fuel pipe. The mesh in the COMSOL® Multiphysics numerical model is tetrahedral whereas, the mesh in the model of IB-Raptor code is Cartesian. The Cartesian mesh is numerically less dissipative than a tetrahedral mesh with analogous characteristics. Moreover, the Cartesian mesh is more consistently refined in the region near the fuel inlet as compared to tetrahedral mesh. Boundary layer mesh in the  $XZ$  section of COMSOL® Multiphysics is finer as compared to the bulk region. Whereas, in IB-Raptor code, the difference in the refinement of the bulk region and boundary layers is negligible in  $XZ$  plane (Figure 10 (b)). The mesh sensitivity study described in the first subsection of 3D non-reactive flow results shows a non-uniformity in the refinement while moving from coarser to finer mesh. In the case of IB-Raptor code the refinement while moving from coarser to finer mesh is more consistent. In summary, to have a closer comparison of two codes, the uniformity in the mesh refinement of two models is required.

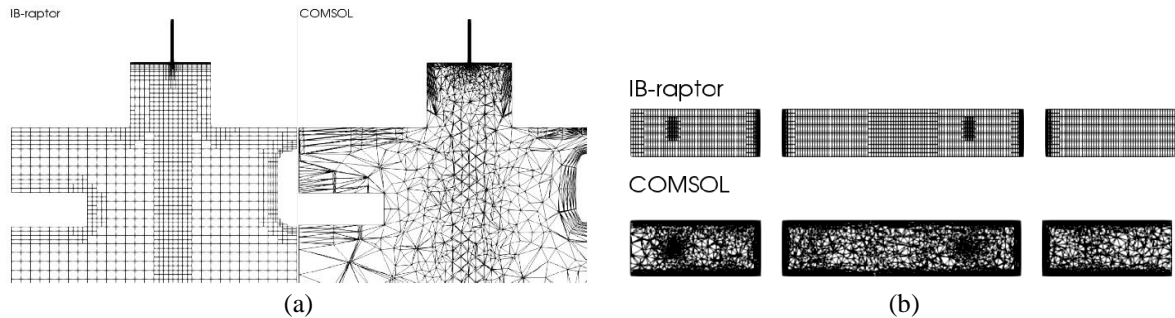


Figure. 10: (a) Comparison of mesh near fuel inlet on  $XY$  center plane with IB-Raptor code and COMSOL® Multiphysics (b) Comparison of mesh on  $XZ$  plane near fuel inlet with IB-Raptor code and COMSOL® Multiphysics

## 4. Conclusion

A 2D reactive turbulent flow model with radiation effects and a 3D non-reactive turbulent flow model of the heating section of an anode baking furnace is studied in this paper. COMSOL<sup>®</sup> Multiphysics software is used for modeling. The effect of radiation studied in the 2D model shows that the temperature is distributed uniformly when the radiation is considered. The strong dependence of thermal NO<sub>x</sub> on temperature distribution necessitates the inclusion of accurate radiation modeling. The temperature calculated by the model is in the range of the temperature measured in the furnace. However, an improved model in terms of combustion and radiation modeling is required to approach the temperature measured in the furnace. A 3D non-reactive turbulent flow model is slightly sensitive to the mesh near fuel inlet as compared to the bulk domain. However, the results do not vary significantly. The results obtained by COMSOL<sup>®</sup> Multiphysics software compares well with IB-Raptor code. The slight differences in the results can be attributed to the dissimilarities in the mesh size and structure. The comparison can be improved further by employing consistency in meshing pattern.

## Acknowledgement

We would like to thank Aluminium & Chemie Rotterdam B.V. for their support.

## References

- [1] D. S. Severo and V. Gusberti, "User-friendly software for simulation of anode baking furnaces," in *Proceeding of the 10th Australasian Aluminum Smelting Technology Conference*, 2011.
- [2] M.J. Bockelie, B.R. Adams, M.A. Cremer, K.A. Davis, E.G. Eddings, J.R. Valentine, P.J. Smith, M.P. Heap "Computational simulations of industrial furnaces," in *American Society of Mechanical Engineers, Pressure Vessels and Piping Division (Publication)*, 1998, pp. 117–124.
- [3] C. K. Westbrook, Y. Mizobuchi, T. J. Poinsot, P. J. Smith, and J. Warnatz, "Computational combustion," *Proc. Combust. Inst.*, 2005.
- [4] E. Dervede, M. A. Thibault, R. T. Bui, and A. Charette, "Simulating the dynamics of the anode baking ring furnace," in *Journal of Metals*, 1984, vol. 36, no. 12, p. 95.
- [5] R. T. Bui, A. Charette, T. Bourgeois, and E. Dervede, "Performance analysis of the ring furnace used for baking industrial carbon electrodes," *Can. J. Chem. Eng.*, vol. 65, no. 1, pp. 96–101, 1987.
- [6] D.S. Severo, V. Gusberti, and P. Elton, "Advanced 3D modelling for anode baking furnaces," *Light Metals 2005*, pp. 697–702, 2005.
- [7] N. Oumarou, D. Kocaefe, Y. Kocaefe, B. Morais, and J. Chabot, "A dynamic process model for simulating horizontal anode baking furnaces," *Mater. Sci. Technol. Conf. Exhib. 2013, MS T 2013*, vol. 3, no. 2013, p. 2077, 2013.
- [8] M. Baiteche, Y. Kocaefe, D. Kocaefe, B. Morais, and J. Laffance, "A 3D mathematical model of a horizontal anode baking furnace as a design tool," *Mater. Sci. Technol. Conf. Exhib. 2013, MS T 2013*, vol. 3, no. 2013, p. 2070, 2013.
- [9] F. Keller and J. H. M. Disselhorst, "Modern Anode Baking Furnace Developments," *Essent. Readings Light Met.*, pp. 486–491, 2013.
- [10] L. Zhang, C. Zheng, and M. Xu, "Simulating the heat transfer process of horizontal anode baking furnace," *Dev. Chem. Eng. Miner. Process.*, vol. 12, no. 3–4, p. 2018, 2004.
- [11] R. T. Bui, E. Dervede, A. Charette, and T. Bourgeois, "Mathematical simulation of a horizontal flue ring furnace," *Essent. Readings Light Met.*, pp. 386–389, 2016.
- [12] A. R. Tajik, T. Shamim, A. F. Ghoniem, and R. K. A. Al-Rub, "CFD modelling of NO<sub>x</sub> and soot formation in aluminum anode baking furnace," p. V08AT10A016, 2019.
- [13] A. R. Tajik, R. K. A. Al-Rub, M. Zaidani, and T. Shamim, "Numerical investigation of turbulent diffusion flame in the aluminum anode baking furnace employing Presumed PDF," *Energy Procedia*, vol. 142, pp. 4157–4162, 2017.
- [14] A. R. Tajik, T. Shamim, R. K. A. Al-Rub, and M. Zaidani, "Two dimensional CFD simulations of a flue-wall in the anode baking furnace for aluminum production," *Energy Procedia*, vol. 105, pp. 5134–5139, 2017.
- [15] P. Nakate, D. J. P. Lahaye, and C. Vuik, "Reactive turbulent flow model of anode baking furnace to estimate NO<sub>x</sub>

through Zeldovich mechanism,” in *Proceedings of the 5th World congress on Mechanical, Chemical and Material Engineering (MCM'19)*, 2019, p. 10.

- [16] H.K. Versteeg, W. Malalasekera, "An introduction to computational fluid dynamics", *Pearson education limited*, Second Edi. 2007.
- [17] T. Poinsot and D. Veynante, "Theoretical and Numerical Combustion", Illustrate. *R.T. Edwards, Inc.*, 2005.
- [18] M. F. Modest and D.C. Haworth, "Radiative heat transfer in turbulent combustion systems: Theory and Applications", Illustrate. *Springer*, 2016.
- [19] J. Donea and A. Huerta, "Finite element methods for flow problem", Illustrate. *John Wiley & Sons*, 2003.
- [20] T. Kangwanpongpan, F. H. R. França, R. Corrêa Da Silva, P. S. Schneider, and H. J. Krautz, "New correlations for the weighted-sum-of-gray-gases model in oxy-fuel conditions based on HITEMP 2010 database," *Int. J. Heat Mass Transf.*, vol. 55, no. 25–26, pp. 7419–7433, 2012.
- [21] "FLIR thermal imaging, night vision and infrared camera systems." [Online]. Available: <https://www.flir.com/>.
- [22] G. Iaccarino and R. Verzicco, "Immersed boundary technique for turbulent flow simulations," *Appl. Mech. Rev.*, vol. 56, no. 3, p. 331, 2003.